ACS APPLIED BIO MATERIALS Cite This: ACS Appl. Bio Mater. 2018, 1, 1687−1694 Article www.acsabm.org

Synthetic Polymer Nanoparticles Functionalized with Different Ligands for Receptor-Mediated Transcytosis across the Blood−Brain Barrier

Qian Lu,[†] Xiaoli Cai,[†] Xian Zhang, Suiqiong Li, Yang Song, Dan Du, Prashanta Dutta,* and Yuehe Lin*

School of Mechanical and Material Engineering, Washington State University, Pullman, Washington 99164, United States

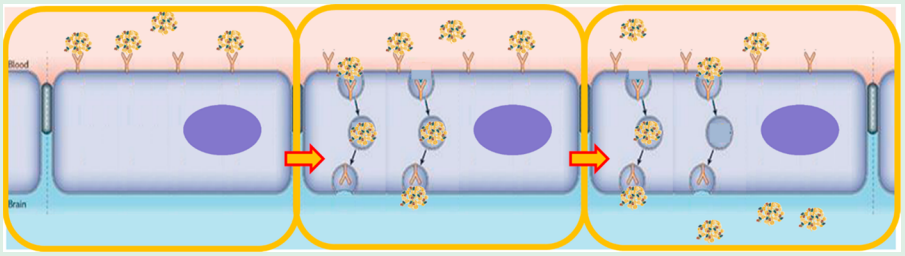

ABSTRACT: Polymeric nanoparticles have been investigated as biocompatible and promising nanocarriers to deliver drugs across the blood−brain barrier (BBB). However, most of the polymeric nanoparticles cannot be observed without attaching them with fluorescent dyes. Generally complex synthesis process is required to attach fluorescent dye tracing molecules with drug carrier nanoparticles. In this paper, we synthesized a novel fluorescent polymer based on poly [Triphenylamine-4-vinyl-(P-methoxy-benzene)] (TEB). This polymeric nanoparticle was prepared from TEB polymer through coprecipitation. Furthermore, three types of ligands, transferrin (TfR), lactoferrin (LfR), and lipoprotein (LRP), were covalently attached on the nanoparticle surface to improve the BBB transport efficiency. All the prepared TEB-based nanoparticles were biocompatible, exhibited excellent fluorescence properties, and could be observed in vivo. The transcellular transportation of these TEB-based nanoparticles across the BBB was evaluated by observing the fluorescent intensity. The translocation study was performed in an in vitro BBB model that were constructed based on mouse cerebral endothelial cells (bEnd.3). The results showed that ligand-coated TEB nanoparticles can be transported across BBB with high efficiencies (up to 29.0%). This is the first time the fluorescent TEB nanoparticles were applied as nanocarriers for transport across the BBB. Such fluorescent polymeric nanoparticles have potential applications in brain imaging or drug delivery.

KEYWORDS: *fluorescence polymer TEB nanoparticles, ligand, blood−brain barrier model, transport efficiency*

INTRODUCTION

The blood−brain barrier (BBB), which is mainly consisting of brain capillary endothelial cells surrounded by pericytes and astrocytes, is a physical barrier that closely maintains and protects the central nervous system of the brain. Unlike the endothelial cells in other organs of the body, the BBB endothelial cells are connected by extensive tight junctions with polarized plasma membrane domains. This tight junction allows nutrients and metabolites to pass through smoothly but restricts the movement of the microscopic objects and large or hydrophilic molecules into the brain from the blood. Even though the BBB is important for the normal function of the central nervous system, this barrier prevents various drug molecules to pass through it. Therefore, finding an effective way that transports the drug molecules across the BBB to reach the target sites is critical for ensuring an effective treatment.

Many strategies have been developed to enhance drug delivery across the BBB, including tight junction modulation of the BBB,[1−5] drug molecule modification[6] and nanoparticle-based drug delivery methods.[7−10] Methods used for BBB cellular junction modulation, such as chemical stimuli,[1] electromagnetic wave impingement,[2] magnetic nanoparticle transportation, and microbubble-assisted focused ultrasound,[3−5] can cause deformation, restructuring or apoptosis of junction proteins, which would potentially endanger the central nervous system.[4,11] For the drug molecule modification, only limited types of small drug molecules can be altered through lipophilic treatments for BBB penetration.[6] Unfortunately, most of the drugs with large molecules cannot be modified. Thus, the scope of tight junction modulation and/or drug molecule modification are very limited for effective drug delivery through the BBB systems. On the other hand, nanoparticle-based drug delivery methods are widely used because they do not cause damages in the BBB structure and are easy to implement through size/charge optimization and surface modification.[12−15] Several types of nanoparticles, such

Received: September 5, 2018
Accepted: October 8, 2018
Published: October 9, 2018

DOI: 10.1021/acsabm.8b00502
ACS Appl. Bio Mater. 2018, 1, 1687−1694

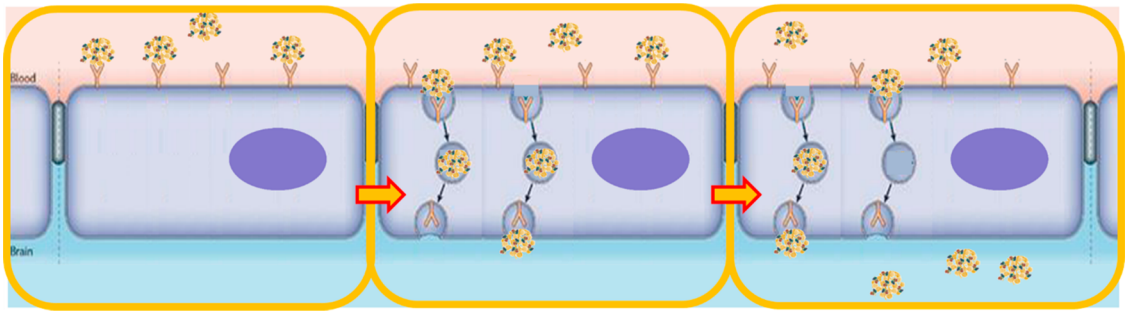

Figure 1. Schematic of receptor-mediated transcytosis pathway across the blood-brain barrier.

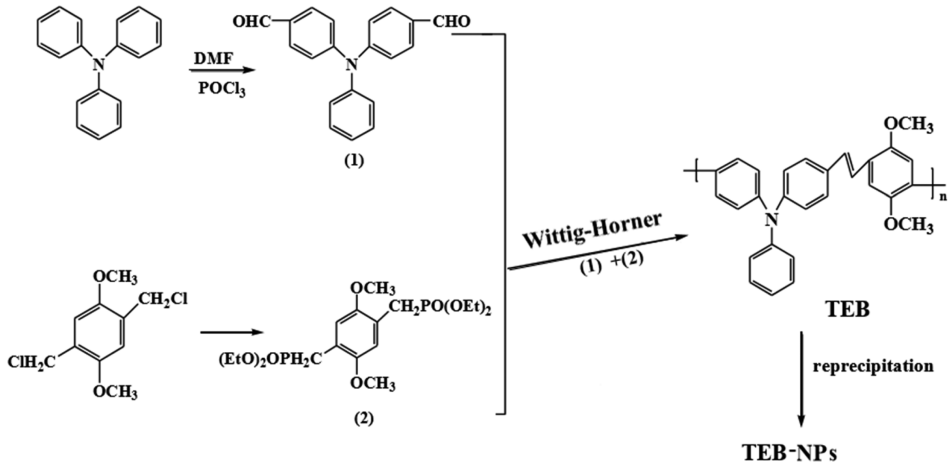

Figure 2. Procedure for the synthesis of the conjugated polymer TEB.

as biological nanoparticles,[16−24] magnetic nanoparticles,[3−5,25] noble metal nanoparticles,[26−31] silica nanoparticles,[32−35] and polymer nanoparticles,[36−43] have been developed for delivering drug across BBB. Over the past decade, polymeric nanoparticles have attracted great attention as effective carriers for delivering targeted drug molecules to brain because they exhibit excellent biocompatibility, good encapsulation and attractive biodegradability.[44,45] Among various polymeric nanoparticles, poly lactic-*co*-glycolic acid (PLGA)-based nanoparticle is the most popular one because of its history of safe use in pharmaceutical industry. For example, Tosi's group used g7 ligand modified PLGA nanoparticles to deliver curcumin into the brain for treatment of Alzheimer's disease (AD).[46] Wang's group developed a new interleukin-6 receptor-mediated PEG−PLGA system for cascade-targeting doxorubicin (DOX) delivery to glioma.[47] However, like these PLGA nanoparticles, currently developed polymeric nanoparticles usually do not have the capability of emitting signals, thus, it is very difficult to (in vivo) observe these nanoparticles directly.[38−43] Recently, Wang's group decorated 1-pyrenecarboxyaldehyde (Pyr) fluorophore onto polymeric nanoparticle for the test strips-based fluorimetric analysis of curcumin and Fe^{3+} ions.[48,49] To study their transcellular transportation, we need to decorate the polymeric nanoparticles with various tracing molecules, such as fluorescent dye molecules, which not only complicate the synthesis process but also change the desired property of the original nanoparticles. Therefore, a novel type of nanoparticles that possesses fluorescence properties and can be used as drug carriers will advance the use of nanoparticles for medical and biological applications.

In this paper, we synthesized a fluorescent polymer, poly [Triphenylamine-4-vinyl-(P-methoxy-benzene)] (TEB) for polymeric nanoparticles. To enhance BBB penetration of nanoparticles, researchers have developed various ligands to conjugate on their surface for receptor-mediated transcytosis (RMT). Among a growing list of ligands, transferrin (TfR), lactoferrin (LfR), and lipoprotein (LRP) have been widely used as receptors in RMT to improve the transcytosis across the BBB.[33,50−53] To achieve RMT (Figure 1) that allows noninvasive and selective delivery of nanoparticle across BBB, we covalently decorated the TEB nanoparticles with these three types of ligands: TfR, LfR, and LRP. All of the prepared TEB-based nanoparticles exhibited excellent fluorescence properties and can be observed in vivo. The transport efficiencies across BBB of different types of TEB-based nanoparticles were investigated. The results showed that ligand-linked TEB nanoparticles could be transported across BBB with high efficiencies.

EXPERIMENTAL SECTION

Materials and Chemistry. All chemicals and solvents, including transferrin, lactoferrin and lipoprotein, were purchased from Sigma-Aldrich. Polycarbonate membrane of transwells (0.4 μm) were obtained from Fisher, USA. Biological reagents for constructing the BBB model, such as fetal bovine serum (FBS), born calf serum, streptomycin, gentamycin and Dulbecco's modified Eagle's medium (DMEM) (ATCC 30−2002), were obtained from ATCC.

Synthesis of Fluorescent TEB Polymer. The synthesis route of the fluorescent TEB polymer was depicted in Figure 2. The two intermediates, 4,4′-diformyl-triphenylamine and 2,5-di-(ethoxyphosphorylene)-1,4-dimethoxybenzene (phospholipid), were synthesized first. The fluorescent TEB polymer was then prepared by

DOI: 10.1021/acsabm.8b00502
ACS Appl. Bio Mater. 2018, 1, 1687−1694

Wittig−Horner reaction. The specific synthesis process is described below.

Synthesis of 4,4′-diformyl-triphenylamine (Intermediate1). Twenty-three milliliters of water-free N,N-dimethylformamide was added into a three-necked flask that was placed in an ice bath with magnetic stirring. In a nitrogen atmosphere, 25 mL of $POCl_3$ was then dropwise added into N,N-dimethylformamide using a constant pressure dropping funnel. When the mixture became a brownish yellow viscous liquid (after about 1 h), 5 g of triphenylamine was put into it and the three-necked flask was moved to an oil bath, and the temperature of the bath was slowly raised to 90 °C. After 4 h, the dark brown reactant was obtained. The reactant was then quickly poured into 500 mL of ice slurry and it was mechanically stirred for 1 h. The prepared product was then fully hydrolyzed, followed by adjusting the pH value of the solution to neutral with NaOH solution (1 mol/L). Subsequently, the solution was extracted with dichloromethane and vacuum filtered. The resulting residue was redissolved into dichloromethane. The organic phase was washed alternately with saturated sodium chloride solution and water. The extract of dichloromethane was treated overnight with anhydrous magnesium sulfate. Finally, the crude product was obtained by vacuum filtering and rotating evaporation. The obtained product was observed using a point plate, and the blue spot was the target product. Using petroleum ether and ethyl acetate (v:v = 2:1) as the developing agent and eluent for silica gel column chromatography, the desired Intermediate1 was obtained with a yield of 80%. ^{1}H NMR (400 MHz, $CDCl_3$) δ (ppm): 9.91 (s, 2H), 7.79 (d, J = 8.2 Hz, 4H), 7.50−7.33 (m, 2H), 7.27 (m, 7H). IR (KBr) ν/cm^{-1}: 2802 cm^{-1}, 2724 cm^{-1} (−CHO, C−H), 1695 cm^{-1} (−CHO, C═O); 1583 cm^{-1}, 1495 cm^{-1}, 1407 cm^{-1} (Ar, C−H).

Synthesis of 2,5-di(Ethoxyphosphorylene)-1,4-dimethoxybenzene (Phospholipid) (Intermediate2). 50 mL of 1,4-dioxane, 10 g of 1,4-dimethoxybenzene and 10 mL of concentrated hydrochloric acid were added into a 250 mL three-necked flask, and then the temperature was slowly increased to 60 °C. Throughout the course of the reaction, HCl gas was continuously bubbled, while the exhaust gas was treated with NaOH solution. Then 10 mL of formaldehyde solution was added in three portions and the solution kept stirring for 3 h. Finally, the reaction system was added into 10 mL of concentrated hydrochloric acid and formaldehyde, respectively. After stirring for 1 h, the resulting solution was cooled down to room temperature. The obtained solid, after suction filtration, was recrystallized from acetone to gain a white reaction intermediate. ^{1}H NMR (400 MHz, DMSO) δ (ppm): 7.13 (s, 2H), 4.67 (d, J = 9.7 Hz, 4H), 3.76 (d, J = 20.5 Hz, 6H).

In a nitrogen atmosphere, 4 g of the above intermediate and 20 mL of triethyl phosphite were put into a 100 mL three-necked flask and heated to 90 °C with stirring at reflux for 1 day. After cooling to room temperature, a white precipitate was obtained. Then it was filtered off with suction to get the crude product which was extracted with trichloromethane and dried with anhydrous $MgSO_4$. After filtering, distillating and washing with$n$-hexane, Intermediate2 was obtained with a yield of 75%. The melting point (Mp) of Intermediate2 was 115 °C. ^{1}H NMR (400 MHz, DMSO) δ (ppm): 6.88 (s, 2H), 3. 92 (m, 8H), 3.73 (d, J = 16.3 Hz, 6H), 3.13 (d, J = 20.2 Hz, 4H), 1.16 (t, J = 7.0 Hz, 12H). Anal. Calcd for: $C_{18}H_{32}O_8P_2$: C, 49.32; H, 7. 31; O, 29.22; P, 14.16; Cl, 9.35; Found: C, 49.45; H, 7.26; O, 29.11; P, 14.18.

Synthesis of the conjugated Poly[triphenylamine-4-vinyl-(P-methoxy-benzene)] (TEB polymer). Under a nitrogen atmosphere, 2.0 mM of Intermediate2 (0. 88 g) and 10 mL of water-free THF were mixed and stirred in an ice bath at 0 °C for 30 min. THF solution containing potassium tertbutoxide (1.3 g) was then added to the above mixture. After stirring for 20 min, the 2.0 mM of Intermediate1 (0.6 g) was added into the reaction system. Subsequently, this mixture was stirred under the protection of nitrogen for 48 h. Finally, vacuum filtering was used to remove the solvent. The residue was then dissolved in dichloromethane and washed with methyl alcohol for three times. The obtained yellow powder was the TEB polymer, with a yield of 50.4%.^{1}H NMR (400 MHz, DMSO) δ (ppm): 7.87−6.43 (m, 17 H), 3.95−3.40 (m, 6 H). IR (KBr) ν/cm^{-1}: 3010 cm^{-1} (=C−H), 1730 cm^{-1} (C═C); 1583 cm^{-1}, 1495 cm^{-1}, 1407 cm^{-1} (Ar, C−H); 1039 cm^{-1}(−OCH_3, C−O). GPC (polystyrene calibration) of TEB with Wittig- Horner reaction by compound 1 and 2: M_w/M_n = 1.389(19%), M_z/M_n = 2.510(40%); M_n = 10690(14%); M_w = 14850(13%); M_z = 26830(37%).

Preparation of TEB-Based Nanoparticles. TEB nanoparticle (TEB-NP) was prepared through the coprecipitation of the TEB polymer. The synthesized TEB powder was first dissolved into THF (1 mg/mL). 50 μL of such solution were then added into 15 mL H_2O/THF solution (V_{H2O}:V_{THF} = 2:1), followed by sonication for 15 min. Subsequently, nitrogen gas was bubbled through the obtained solution to remove THF and H_2O. As the THF and H_2O evaporated, the polymer molecules began to agglomerate to form nanoparticles. When the solution was reduced to 5 mL volume, it was considered that all polymer molecules were consumed and the polymeric nanoparticle solution (10 ug/mL) was obtained. To link different ligands on the nanoparticles, we first modified the nanoparticle surfaces with COOH group (TEB-NP-COOH). For the synthesis of TEB-NP-COOH, 50 μL of TEB/THF (1 mg/mL) was mixed with 20 μL poly(styrene-*co*-maleic anhydride)(PSMA)/THF (1 mg/mL), and then was added into 15 mL H_2O/THF solution (V_{H2O}:V_{THF} = 2:1). By following the subsequent procedures described above, TEB-NP-COOH solution (10 ug/mL) was obtained.

Three types of ligands, transferrin (TfR), lactoferrin (LfR), and lipoprotein (LRP), were covalently attached to TEB-NP-COOH to form three different nanoparticles (Figure 3). To link the ligands on

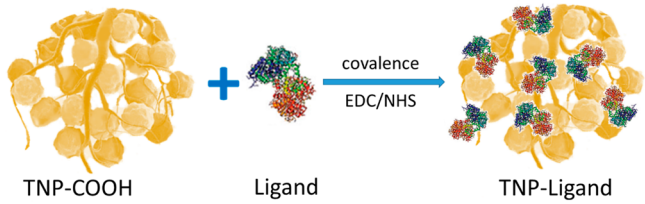

Figure 3. Scheme of linkage of the ligand to the polymer nanoparticles.

the nanoparticles, the nanoparticle surfaces need to be activated first. One milliliter of the as-prepared TEB-NP-COOH solution (10 ug/mL) was mixed 30 μL of 1-(3-(Dimethylamino)propyl)-3-ethylcarbodiimide hydrochloride (EDC, 5 mg/mL) and incubated for 2 h. Subsequently, 20 μL of 1-hydroxypyrrolidine-2,5-dione (NHS, 5 mg/mL) was added and incubated for 30 min. After the surface activation, 40 μL of each ligand solution (TfR, LfR, LRP, 1 mg/mL) was mixed with the nanoparticle solution, respectively. These mixed solutions were stirred for 24 h. Finally, the ligand-linked nanoparticles, TEB-NP-TfR, TEB-NP-LfR, and TEB-NP-LRP, were obtained.

Characterization of TEB-Based Nanoparticles. Philips CM200 UT (Field Emission Instruments, USA) were used to obtain transmission electron microscopy (TEM) images. The ultraviolet−visible (UV−vis) absorption spectra were achieved using a Genesys 10s Bio UV/Visible Spectrophotometer (Thermo Scientific, USA). Zeta potentials of the prepared nanoparticles were measured on a Malvern Zetasizer Nano ZS90 (Malvern Instruments Ltd., UK). Fluorescence spectrum analysis of the nanoparticles were performed using a FluoroMax 4 spectorfluorometer (Horiba, Japan).

Evaluation of the Biocompatibility of the TEB-Based Systems. The in vitro cytotoxicity of all synthesized nanoparticles (TEB-NP, TEB-NP-COOH, TEB-NP-TfR, TEB-NP-LfR and TEB-NP-LRP) against mouse cerebral endothelial cells (bEnd.3) was measured using a standard 3-(4,5-dimethylthiazol-2-yl)-2,5-diphenylte-trazolium (MTT) method. The bEnd.3 cells were planted in a 96-well plate (1 × 10^5 cells per well). After 24 h incubation, the bEnd.3 cells were treated with DMEM medium containing different concentrations of polymer nanoparticles, followed by incubation for 1 day. Then 10 μL of MTT solution (Fisher, 5.0 mg mL^{-1} in PBS) were

DOI: 10.1021/acsabm.8b00502
ACS Appl. Bio Mater. 2018, 1, 1687−1694

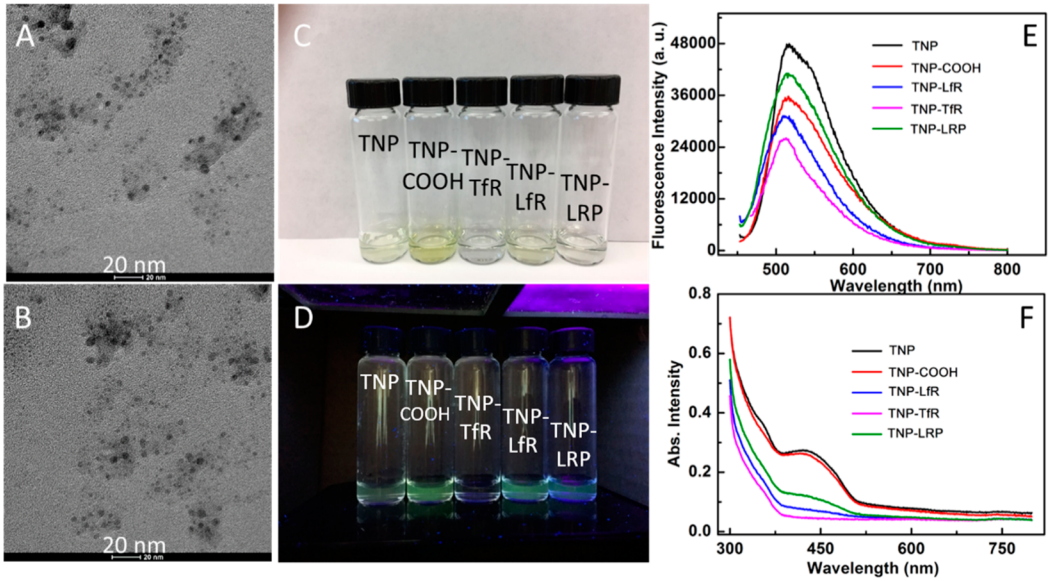

Figure 4. TEM imaging of (A) TEB-NP and (B) TEB-NP-COOH. Image of TEB-based nanoparticles in aqueous solutions were taken under (C) sunlight and (D) 365 nm ultraviolet lamp. (E) Photoluminescence for the same concentration of polymer nanoparticles (excitation 435 nm). (F) UV−vis absorption spectra of polymer nanoparticles.

added into each well containing fresh culture medium. After incubating for another 4 h, 100 μL of dimethyl sulfoxide (DMSO) was added into each well. Finally, a Synergy H1 microplate reader (BioTeK, Winooski, VT) was used to read the optical density of each sample (540 nm wavelength). The relative cell viability (%) was calculated by $(A_{test}/A_{control}) \times 100\%$ and the experiments were repeated three times.

Construction of in Vitro BBB Model. Our in vitro BBB model was constructed based on mice endothelial cells (bEnd.3 cell) since the vascular structures in humans and mice are remarkably similar at a physiological level. The bEnd.3 cells were planted on the microporous membranes (0.4 μm) of transwell inserts (1×10^5 cells/well), which were placed into a 6-well plate. Next, 2.00 and 2.75 mL of DMEM medium were added to the apical side and the basolateral side of each transwell, respectively. The cells were cultured in a humidified incubator (37 °C, 5% CO_2) and the DMEM medium were refreshed every 24 h. After culturing for 12 days, the BBB model was formed.

Evaluation of the in Vitro BBB Model Function. The integrity of the formed BBB model was determined by measuring the trans-endothelial electrical resistance (TEER) of the barrier using an EVOM voltmeter (10 μA current at 12.5 Hz). The measurement was performed by placing the detecting electrodes at the basolateral side and the apical side of the transwell and recording the resistance upon an applied potential. The TEER value of the barrier layer was calculated by the following eq 1.

$$\text{TEER} = (R_t - R_b)A \quad (1)$$

where R_t is the measured resistance of the cell culture membrane and R_b is the resistance of the fresh polycarbonate membrane of the transwell insert without cell culture; A is the area of the transwell insert membrane.

Determination of the BBB Transport Efficiency of the TEB-Based Nanoparticles. Because TEB-based nanoparticles are fluorescent themselves, their BBB transport efficiency can be determined by directly measuring the fluorescence intensities of the particles in the medium at the two sides of the BBB. We investigated the BBB transport efficiencies of 5 types of the TEB-based nanoparticles: TEB-NP, TEB-NP-COOH, TEB-NP-TfR, TEB-NP-LfR, and TEB-NP-LRP. For each type of nanoparticles, the fluorescence intensity of TEB-based nanoparticles is linearly related with the concentration of TEB-based nanoparticles. Therefore, the BBB transport efficiency was evaluated by directly measuring the fluorescence intensity changes at the apical and basolateral side in the BBB model. For each type of the TEB-based nanoparticles, the fluorescent intensity of the nanoparticles was first recorded for a concentration of 0.5 μg/mL. The nanoparticles were then added into the apical side of the BBB model. In the fluorescent analysis, the pure DMEM medium without nanoparticles was used as the blank. After 12 h incubation, the medium in the basolateral side was gathered and its fluorescent intensity was measured.

The transport efficiency of TEB-based nanoparticles across the BBB model was then calculated using the following equation:

$$\text{transport efficiency (\%)} = (I_b - I_c)100/(I_t - I_c) \quad (2)$$

where I_b and I_t are the fluorescence intensity of the collected basolateral medium after the TEB-based nanoparticles are incubated in the BBB model for 12 h and the medium with original concentration of the nanoparticles (0.5 μg/mL) at the apical side, respectively. I_c is the fluorescent intensity of blank DMEM medium without any nanoparticle.

RESULTS AND DISCUSSION

Characterization of TEB-Based Systems. All of the synthesized nanoparticles, TEB-NP, TEB-NP-COOH and ligand-linked TEB nanoparticles, were highly stable in water without any agglomeration (Figure 4C). Figure 4(A, B) present the TEM images of TEB-NP and TEB-NP-COOH, respectively, which reveal that both types of the nanoparticles were roughly spherical in shape with average diameters of 25 nm. The results show that carboxyl functional modification does not alter the particle size and morphology of the polymer nanoparticles. Many studies have investigated the effect of the nanoparticle size on the BBB transport efficiency. Some of the results indicated that an increase in the particle size resulted in a decrease in the permeation efficiency of the nanoparticle across the BBB.[54] The 25 nm nanoparticles had maximum transport efficiency to cross the BBB.[33,54,55] Therefore, the prepared TEB-based nanoparticles with such size were favorable for transportation across the BBB.

Since TEB is a type of fluorescent polymer, the TEB-based nanoparticles exhibit excellent fluorescent properties. All of the TEB-based nanoparticles emitted green luminescence when excited under 365 nm ultraviolet light (Figure 4D). The UV−

DOI: 10.1021/acsabm.8b00502
ACS Appl. Bio Mater. 2018, 1, 1687−1694

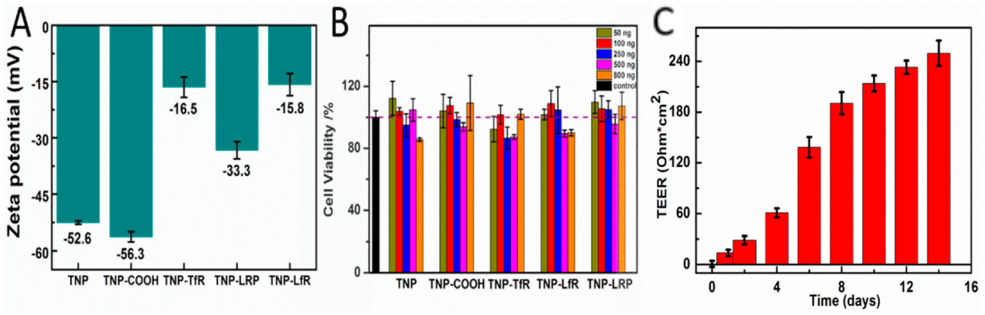

Figure 5. (A) Zeta potential analysis of TEB-based nanoparticles at a concentration of 5.0 μg/mL. (B) Cytotoxicity of TEB-based nanoparticles in bEnd.3 cells. (C) The trans-endothelial electrical resistance (TEER) values of the BBB models during cell culture. The error bars show the standard deviation of TEER values.

vis spectra of the TEB-based nanoparticles in aqueous solutions were presented in Figure 4F. For all of the TEB-based nanoparticles, the absorption peaks were centered at approximately 435 nm, which could be identified as the characteristic absorption peak of the TEB polymeric nanoparticle. The surface decoration of the nanoparticles does not affect the absorption wavelength of the nanoparticles. Figure 4E shows the fluorescent emission spectra of different types of the TEB-based nanoparticles under 435 nm excitation wavelength. The emission peak wavelengths of different TEB-based nanoparticles were found to be constant at 515 nm. The TEB-NP exhibited highest emission intensity compared with other types of TEB-nanoparticles. After modified with COOH group or different ligands, the fluorescent intensities of the nanoparticles decreased. For TEB-NP-TfR, the fluorescent intensity reduced almost 50% compared with TEB-NP.

The zeta potentials of the prepared nanoparticles varied based on their surface modifications. TEB-NP possessed a negative zeta potential of −52.6 mV (Figure 5A). TEB-NP-COOH showed an even more negative zeta potential (−56.3 mV) due to the carboxylic group. On the other hand, attaching different ligands on the nanoparticles significantly increased the zeta potentials. Compared to the TEB-NP, the zeta potentials for ligand-linked TEB nanoparticles are much more close to neutral potential, which is favorable for the nanoparticles penetrating through the BBB membrane.[6−8,56]

Biocompatibility of TEB-Based Nanoparticles. The cytotoxicity of the TEB-based nanoparticles was evaluated by the standard MTT assay[57,58] with bEnd.3 cells. As shown in Figure 5B, when concentrations up to 800 ng mL^{-1}, TEB-NP and TEB-NP-COOH nanoparticles showed no obvious effect on cell viability. For ligand modified TEB-based nanoparticles (TEB-NP-TfR, TEB-NP-LfR, and TEB-NP-LRP), more than 90% of the cells survived after 24 h incubation at concentrations ranging from 50 to 800 ng mL^{-1}. These results indicated that TEB-based nanoparticles have low cytotoxicity and therefore could be used to develop safe nanoprobes/nanocarriers for biological and medical applications.

Structure Integrity of BBB Model. The trans-endothelial electrical resistance (TEER) value is an important parameter to assess the integrity of the BBB model and its barrier properties. The formation of the tight junctions between neighboring endothelial cell results in an extremely high electric resistance, which could reach up to 200 Ω cm^2 within 8−12 days of cell culturing.[33,59] The TEER value is directly correlated with the permeability of BBB for transportation of extracellular molecule.[60] As shown in Figure 5C, the measured TEER value across the transwell insert membrane increased with the increase in the incubation time, indicating the continuous formation of the tight junctions between endothelial cells. A TEER value of 233 Ω cm^2 was obtained after 12 days of incubation, which showed that an in vitro BBB model was constructed and could be applied to investigate the transportation of the prepared nanoparticles.

Receptor-Mediated Transcytosis of TEB-Based Systems Across in Vitro BBB. The internalization efficiency of the TEB-based nanoparticles into living cells was first analyzed with bEnd.3 cells as a model. The TEB-based nanoparticles were incubated with bEnd.3 cells and the intercellular fluorescent images of the nanoparticles were characterized. As shown in the images taking by a confocal microscopy (Figure 6A−E), TEB-NP and TEB-NP-COOH show negligible cell uptake in bEnd.3 cells. On the other hand, ligand-decorated TEB-based nanoparticles exhibit a selective and more efficient internalization into bEnd.3 cells. The fluorescence intensities of the TEB-based nanoparticles attached with ligands inside the bEnd.3 cells are significantly stronger than TEB-NP and TEB-NP-COOH. This result showed that the ligands improved the uptake efficiency of TEB-based nano particles.

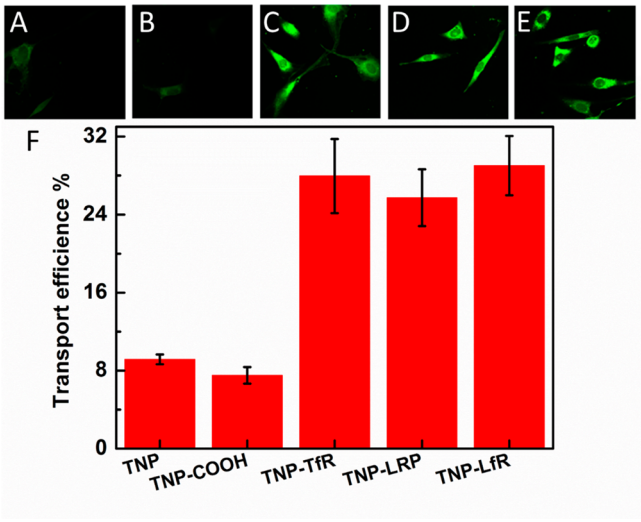

Figure 6. Confocal images of the bEnd.3 cells treated with (A) TEB-NP, (B) TEB-NP-COOH, (C) TEB-NP-TfR, (D) TEB-NP-LRP, and (E) TEB-NP-LfR. (F) Transport efficiencies of TEB-based polymeric nanoparticles across the in vitro BBB model.

DOI: 10.1021/acsabm.8b00502
ACS Appl. Bio Mater. 2018, 1, 1687−1694

With the assistance of the ligands, the TEB-based nanoparticles penetrate across BBB through transcytosis. Figure 6 represents the transportation efficiencies across BBB for all prepared nanoparticles. Without any surface modification, the pure TEB-NP shows a BBB transportation efficiency of about 9.2%. The endothelial cell membrane has a lipid-based bilayer membrane structure, which allows the lipophilic substances to pass easily. Therefore, a high liposolubility of nanoparticles is beneficial for their ability to penetrate across the BBB. The TEB-based nanoparticles have lipophilic surfaces that are favorable for penetrating the BBB. However, the high electronegativity of TEB-NP limited its transport efficiency. Similarly, the transportation efficiency of TEB-NP-COOH was further reduced to 7.5% since the surface modification of the carboxyl group increased the electronegativity of the nanoparticles. On the other hand, the transportation efficiencies of TEB-NP-TfR, TEB-NP-LRP and TEB-NP-LfR were 28.0%, 25.7%, and 29.0%, respectively. The significant improvement of the BBB transportation efficiencies for ligand-linked nanoparticles can be attributed to two factors. First, the relatively low zeta potentials of the ligand-modified nanoparticles allow them to pass through the BBB membrane easily. Second, the attached ligands act as anchoring target for receptors that improve the selectivity and affinity of the nanoparticles toward the endothelial cells, resulting in better uptake and penetration rates. By attaching with proper ligands, TEB-based polymeric nanoparticles can effectively transport across BBB through receptor-mediated transcytosis.

CONCLUSION

In summary, a fluorescent polymer, TEB, was successfully synthesized. TEB-based nanoparticles were prepared based on coprecipitation of TEB molecules. Three types of ligand-linked TEB-based nanoparticles, TEB-NP-TfR, TEB-NP-LfR, and TEB-NP-LRP were prepared by covalently attaching TfR, LfR, and LRP on the carboxyl-functionalized TEB nanoparticles, respectively. Characterization showed that TEB-based nanoparticles exhibited excellent fluorescent properties, and the fluorescent intensities of TEB-based nanoparticles linearly increased with their concentrations. Thus, the transcellular transportation of these nanoparticles can be in vivo analyzed using fluorescence imaging. In this study, an in vitro BBB model was constructed by culturing mouse cerebral endothelial cells (bEnd.3) on transwell inserts. The transport efficiencies across BBB for different types of TEB-based nanoparticles were investigated. The results showed that ligand-linked TEB nanoparticles transport across BBB through receptor-mediated transcytosis, and high transport efficiencies (up to 29.0%) were achieved for LfR receptors. The TEB-based fluorescent nanoparticles developed in this work are easy to observe, which have great potential for applications, such as drug delivery, brain-imaging, brain disease diagnosis, and treatment.

AUTHOR INFORMATION

Corresponding Authors

*E-mail: yuehe.lin@wsu.edu. Fax: 5093354662 (Y.L.).
*E-mail: prashanta@wsu.edu (P.D.).

ORCID

Yang Song: 0000-0003-0848-4831
Dan Du: 0000-0003-1952-4042
Yuehe Lin: 0000-0003-3791-7587

Author Contributions

†Q.L. and X.C. contributed equally to this work.

Notes

The authors declare no competing financial interest.

ACKNOWLEDGMENTS

The research reported in this publication was supported by the National Institute of General Medical Sciences of the National Institutes of Health under award number R01GM122081. The content is solely the responsibility of the authors and does not necessarily represent the official views of the National Institutes of Health.

REFERENCES

(1) Orive, G.; Ali, O. A.; Anitua, E.; Pedraz, J. L.; Emerich, D. F. Biomaterial-Based Technologies for Brain Anti-cancer Therapeutics and Imaging. *Biochim. Biophys. Acta, Rev. Cancer* **2010**, *1806*, 96−107.
(2) Gao, J.; Gu, H.; Xu, B. Multifunctional Magnetic Nanoparticles: Design, Synthesis, and Biomedical Applications. *Acc. Chem. Res.* **2009**, *42*, 1097−1107.
(3) Tran, N.; Webster, T. J. Magnetic Nanoparticles: Biomedical Applications and Challenges. *J. Mater. Chem.* **2010**, *20*, 8760−8767.
(4) Gupta, A. K.; Naregalkar, R. R.; Vaidya, V. D.; Gupta, M. Recent Advances on Surface Engineering of Magnetic Iron Oxide Nanoparticles and Their Biomedical Applications. *Nanomedicine* **2007**, *2*, 23−39.
(5) Neuberger, T.; Schöpf, B.; Hofmann, H.; Hofmann, M.; von Rechenberg, B. Superparamagnetic Nanoparticles for Biomedical Applications: Possibilities and Limitations of A New Drug Delivery System. *J. Magn. Magn. Mater.* **2005**, *293*, 483−496.
(6) Lockman, P. R.; Mumper, R. J.; Khan, M. A.; Allen, D. D. Nanoparticle Technology for Drug Delivery Across the Blood-Brain Barrier. *Drug Dev. Ind. Pharm.* **2002**, *28*, 1−13.
(7) Lockman, P. R.; Koziara, J. M.; Mumper, R. J.; Allen, D. D. Nanoparticle Surface Charges Alter Blood-Brain Barrier Integrity and Permeability. *J. Drug Targeting* **2004**, *12*, 635−641.
(8) Schroeder, U.; Sommerfeld, P.; Ulrich, S.; Sabel, B. A. Nanoparticle Technology for Delivery of Drugs Across the Blood−Brain Barrier. *J. Pharm. Sci.* **1998**, *87*, 1305−1307.
(9) Yoshikawa, T.; Sakaeda, T.; Sugawara, T.; Hirano, K.; Stella, V. J. A Novel Chemical Delivery System for Brain Targeting. *Adv. Drug Delivery Rev.* **1999**, *36*, 255−275.
(10) Gidwani, M.; Singh, A. V. Nanoparticle Enabled Drug Delivery Across the Blood Brain Barrier: in Vivo and in Vitro Models, Opportunities and Challenges. *Curr. Pharm. Biotechnol.* **2014**, *14*, 1201−1212.
(11) Li, Z.; Barnes, J. C.; Bosoy, A.; Stoddart, J. F.; Zink, J. I. Mesoporous Silica Nanoparticles in Biomedical Applications. *Chem. Soc. Rev.* **2012**, *41*, 2590−2605.
(12) Wohlfart, S.; Gelperina, S.; Kreuter, J. Transport of Drugs Across the Blood-Brain Barrier by Nanoparticles. *J. Controlled Release* **2012**, *161*, 264−273.
(13) Saraiva, C.; Praça, C.; Ferreira, R.; Santos, T.; Ferreira, L.; Bernardino, L. Nanoparticle-Mediated Brain Drug Delivery: Overcoming Blood-Brain Barrier to Treat Neurodegenerative Diseases. *J. Controlled Release* **2016**, *235*, 34−47.
(14) Grabrucker, A. M.; Ruozi, B.; Belletti, D.; Pederzoli, F.; Forni, F.; Vandelli, M. A.; Tosi, G. Nanoparticle Transport Across the Blood Brain Barrier. *Tissue Barriers* **2016**, *4*, No. e1153568.
(15) Bode, G. H.; Coué, G.; Freese, C.; Pickl, K. E.; Sanchez-Purrà, M.; Albaiges, B.; Borrós, S.; Van Winden, E. C.; Tziveleka, L. A.; Sideratou, Z.; Engbersen, J. F. J.; Singh, S.; Albrecht, K.; Groll, J.; Möller, M.; Pötgens, A. J. G.; Schmitz, C.; Fröhlich, E.; Grandfils, C.; Sinner, F. M.; Kirkpatrick, C. J.; Steinbusch, H. W. M.; Frank, H. G.; Unger, R. E.; Martinez-Martinez, P. An in vitro and in vivo Study of Peptide-Functionalized Nanoparticles for Brain Targeting: The

DOI: 10.1021/acsabm.8b00502
ACS Appl. Bio Mater. 2018, 1, 1687−1694

Importance of Selective Blood-Brain Barrier Uptake. *Nanomedicine* **2017**, *13*, 1289−1300.
(16) Gu, J.; Al-Bayati, K.; Ho, E. A. Development of Antibody-Modified Chitosan Nanoparticles for the Targeted Delivery of siRNA Across the Blood-Brain Barrier as a Strategy for Inhibiting HIV Replication in Astrocytes. *Drug Delivery Transl. Res.* **2017**, *7*, 497−506.
(17) Lin, T. T.; Zhao, P. F.; Jiang, Y. F.; Tang, Y. S.; Jin, H. Y.; Pan, Z. Z.; He, H. N.; Yang, V.; Huang, Y. Z. Blood-Brain-Barrier-Penetrating Albumin Nanoparticles for Biomimetic Drug Delivery via Albumin-Binding Protein Pathways for Antiglioma Therapy. *ACS Nano* **2016**, *10*, 9999−10012.
(18) Sahin, A.; Yoyen-Ermis, D.; Caban-Toktas, S.; Horzum, U.; Aktas, Y.; Couvreur, P.; Esendagli, G.; Capan, Y. Evaluation of Brain-Targeted Chitosan Nanoparticles Through Blood-Brain Barrier Cerebral Microvessel Endothelial Cells. *J. Microencapsulation* **2017**, *34*, 659−666.
(19) Varga, N.; Csapó, E.; Majláth, Z.; Ilisz, I.; Krizbai, I. A.; Wilhelm, I.; Knapp, L.; Toldi, J.; Vécsei, L.; Dékány, I. Targeting of the Kynurenic Acid Across the Blood-Brain Barrier by Core-Shell Nanoparticles. *Eur. J. Pharm. Sci.* **2016**, *86*, 67−74.
(20) Gomes, M. J.; Dreier, J.; Brewer, J.; Martins, S.; Brandl, M.; Sarmento, B. A New Approach for A Blood-Brain Barrier Model Based on Phospholipid Vesicles: Membrane Development and siRNA-Loaded Nanoparticles Permeability. *J. Membr. Sci.* **2016**, *503*, 8−15.
(21) Lin, T.; Zhao, P.; Jiang, Y.; Tang, Y.; Jin, H.; Pan, Z.; He, H.; Yang, V. C.; Huang, Y. Blood-Brain-Barrier-Penetrating Albumin Nanoparticles for Biomimetic Drug Delivery via Albumin-Binding Protein Pathways for Antiglioma Therapy. *ACS Nano* **2016**, *10*, 9999−10012.
(22) Dal Magro, R.; Ornaghi, F.; Cambianica, I.; Beretta, S.; Re, F.; Musicanti, C.; Rigolio, R.; Donzelli, E.; Canta, A.; Ballarini, E.; Cavaletti, G.; Gasco, P.; Sancini, G. ApoE-Modified Solid Lipid Nanoparticles: A Feasible Strategy to Cross the Blood-Brain Barrier. *J. Controlled Release* **2017**, *249*, 103−110.
(23) Rehman, M.; Madni, A.; Shi, D.; Ihsan, A.; Tahir, N.; Chang, K. R.; Javed, I.; Webster, T. J. Enhanced Blood Brain Barrier Permeability and Glioblastoma Cell Targeting via Thermoresponsive Lipid Nanoparticles. *Nanoscale* **2017**, *9*, 15434−15440.
(24) Alexis, F.; Pridgen, E. M.; Langer, R.; Farokhzad, O. C. Nanoparticle Technologies for Cancer Therapy. *Handb. Exp. Pharmacol.* **2010**, *197*, 55−86.
(25) Ghadiri, M.; Vasheghani-Farahani, E.; Atyabi, F.; Kobarfard, F.; Mohamadyar-Toupkanlou, F.; Hosseinkhani, H. Transferrin-Conjugated Magnetic Dextran-Spermine Nanoparticles for Targeted Drug Transport Across Blood-Brain Barrier. *J. Biomed. Mater. Res., Part A* **2017**, *105*, 2851−2864.
(26) Ruff, J.; Hüwel, S.; Kogan, M. J.; Simon, U.; Galla, H. J. The Effects of Gold Nanoparticles Functionalized with ß-amyloid Specific Peptides on An in vitro Model of Blood-Brain Barrier. *Nanomedicine* **2017**, *13*, 1645−1652.
(27) Zhang, Y.; Walker, J. B.; Minic, Z.; Liu, F.; Goshgarian, H.; Mao, G. Transporter Protein and Drug-Conjugated Gold Nanoparticles Capable of Bypassing the Blood-Brain Barrier. *Sci. Rep.* **2016**, *6*, 25794−25802.
(28) Chen, I.-C.; Hsiao, I.-L.; Lin, H.-C.; Wu, C.-H.; Chuang, C.-Y.; Huang, Y.-J. Influence of Silver and Titanium Dioxide Nanoparticles on in vitro Blood-Brain Barrier Permeability. *Environ. Toxicol. Pharmacol.* **2016**, *47*, 108−118.
(29) Lin, H.-C.; Ho, M.-Y.; Tsen, C.-M.; Huang, C.-C.; Wu, C.-C.; Huang, Y.-J.; Hsiao, I.-L.; Chuang, C.-Y. Comparative Proteomics Reveals Silver Nanoparticles Alter Fatty Acid Metabolism and Amyloid Beta Clearance for Neuronal Apoptosis in a Triple Cell Coculture Model of the Blood−Brain Barrier. *Toxicol. Sci.* **2017**, *158*, 151−163.
(30) Sokołowska, P.; Białkowska, K.; Siatkowska, M.; Rosowski, M.; Kucińska, M.; Komorowski, P.; Makowski, K.; Walkowiak, B. Human Brain Endothelial Barrier Cells are Distinctly Less Vulnerable to Silver Nanoparticles Toxicity than Human Blood Vessel Cells: A Cell-specific Mechanism of the Brain Barrier? *Nanomedicine* **2017**, *13*, 2127−2130.
(31) Wang, P.; Wang, C.; Lu, L.; Li, X.; Wang, W.; Zhao, M.; Hu, L.; El-Toni, A. M.; Li, Q.; Zhang, F. Kinetics-mediate Fabrication of Multi-model Bioimaging Lanthanide Nanoplates with Controllable Surface Roughness for Blood Brain Barrier Transportation. *Biomaterials* **2017**, *141*, 223−232.
(32) Baghirov, H.; Karaman, D.; Viitala, T.; Duchanoy, A.; Lou, Y.-R.; Mamaeva, V.; Pryazhnikov, E.; Khiroug, L.; de Lange Davies, C.; Sahlgren, C.; Rosenholm, J. M. Feasibility Study of the Permeability and Uptake of Mesoporous Silica Nanoparticles across the Blood-Brain Barrier. *PLoS One* **2016**, *11* (8), No. e0160705.
(33) Song, Y.; Du, D.; Li, L.; Xu, J.; Dutta, P.; Lin, Y. In Vitro Study of Receptor-Mediated Silica Nanoparticles Delivery across Blood-Brain Barrier. *ACS Appl. Mater. Interfaces* **2017**, *9*, 20410−20416.
(34) Liu, D.; Lin, B. Q.; Shao, W.; Zhu, Z.; Ji, T. H.; Yang, C. Y. In Vitro and in Vivo Studies on the Transport of PEGylated Silica Nanoparticles across the Blood-Brain Barrier. *ACS Appl. Mater. Interfaces* **2014**, *6*, 2131−2136.
(35) Liu, X.; Sui, B.; Sun, J. Blood-Brain Barrier Dysfunction Induced by Silica NPs in vitro and in vivo: Involvement of Oxidative Stress and Rho-kinase/JNK Signaling Pathways. *Biomaterials* **2017**, *121*, 64−82.
(36) Gomes, M. J.; Fernandes, C.; Martins, S.; Borges, F.; Sarmento, B. Tailoring Lipid and Polymeric Nanoparticles as siRNA Carriers towards the Blood-Brain Barrier - from Targeting to Safe Administration. *J. Neuroimmune Pharmacol* **2017**, *12*, 107−119.
(37) Monaco, I.; Camorani, Simona.; Colecchia, D.; Locatelli, E.; Calandro, P.; Oudin, A.; Niclou, S.; Arra, C.; Chiariello, M.; Cerchia, L.; Comes Franchini, M. Aptamer Functionalization of Nanosystems for Glioblastoma Targeting through the Blood-Brain Barrier. *J. Med. Chem.* **2017**, *60*, 4510−4516.
(38) Baysal, I.; Ucar, G.; Gultekinoglu, M.; Ulubayram, K.; Yabanoglu-Ciftci, S. Donepezil loaded PLGA-b-PEG Nanoparticles: Their Ability to Induce Destabilization of Amyloid Fibrils and to Cross Blood Brain Barrier in vitro. *J. Neural Transm* **2017**, *124*, 33−45.
(39) Kuo, Y.-C.; Rajesh, R. Targeted Delivery of Rosmarinic Acid Across the Blood-Brain Barrier for Neuronal Rescue Using Polyacrylamide-chitosan-poly(lactide-co-glycolide) Nanoparticles with Surface Cross-reacting Material 197 and Apolipoprotein E. *Int. J. Pharm.* **2017**, *528*, 228−241.
(40) Kou, L.; Hou, Y.; Yao, Q.; Guo, W.; Wang, G.; Wang, M.; Fu, Q.; He, Z. L-Carnitine-Conjugated Nanoparticles to Promote Permeation Across Blood-Brain Barrier and to Target Glioma Cells for Drug Delivery via the Novel Organic Cation/ Carnitine Transporter OCTN2. *Artif. Cells, Nanomed., Biotechnol.* **2017**, *3*, 1−12.
(41) Bhowmik, A.; Chakravarti, S.; Ghosh, A.; Shaw, R.; Bhandary, S.; Bhattacharyya, S.; Sen, P. C.; Ghosh, M. K. Anti-SSTR2 Peptide Based Targeted Delivery of Potent PLGA Encapsulated 3,3′-diindolylmethane Nanoparticles Through Blood Brain Barrier Prevents Glioma Progression. *Oncotarget* **2017**, *8*, 65339−65358.
(42) Barbara, R.; Belletti, D.; Pederzoli, F.; Masoni, M.; Keller, J.; Ballestrazzi, A.; Vandelli, M. A.; Tosi, G.; Grabrucker, A. M. Novel Curcumin Loaded Nanoparticles Engineered for Blood-Brain Barrier Crossing and Able to Disrupt Abeta Aggregates. *Int. J. Pharm.* **2017**, *526*, 413−424.
(43) Shi, W.; Cui, X.; Shi, J.; Chen, J.; Wang, Y. Overcoming the Blood-Brain Barrier for Glioma-targeted Therapy Based on an Interleukin-6 Receptor-Mediated Micelle System. *RSC Adv.* **2017**, *7*, 27162−27169.
(44) Quader, S.; Liu, X.; Chen, Y.; Mi, P.; Chida, T.; Ishii, T.; Miura, Y.; Nishiyama, N.; Cabral, H.; Kataoka, K. cRGD Peptide-Installed Epirubicin-Loaded Polymeric Micelles for Effective Targeted Therapy Against Brain Tumors. *J. Controlled Release* **2017**, *258*, 56−66.
(45) Zhang, C.; Nance, E. A.; Mastorakos, P.; Chisholm, J.; Berry, S.; Eberhart, C.; Tyler, B.; Brem, H.; Suk, J.; Hanes, J. Convection

DOI: 10.1021/acsabm.8b00502
ACS Appl. Bio Mater. 2018, 1, 1687−1694

Enhanced Delivery of Cisplatin-Loaded Brain Penetrating Nanoparticles Cures Malignant Glioma in Rats. *J. Controlled Release* **2017**, *263*, 112−119.
(46) Barbara, R.; Belletti, D.; Pederzoli, F.; Masoni, M.; Keller, J.; Ballestrazzi, A.; Vandelli, M. A.; Tosi, G.; Grabrucker, A. M. Novel Curcumin Loaded Nanoparticles Engineered for Blood-Brain Barrier Crossing and Able to Disrupt Abeta Aggregates. *Int. J. Pharm.* **2017**, *526*, 413−424.
(47) Shi, W.; Cui, X. X.; Shi, J. L.; Chen, J.; Wang, Y. Overcoming the Blood-Brain Barrier for Glioma-Targeted Therapy Based on An Interleukin-6 Receptor-Mediated Micelle System. *RSC Adv.* **2017**, *7*, 27162−27169.
(48) Duan, Z. Q.; Yin, M. Y.; Zhang, C. X.; Song, G. L.; Zhao, S. Y.; Yang, F.; Feng, L. P.; Fan, C.; Zhu, S. Y.; Wang, H. Polyhydric Polymer-Loaded Pyrene Composites as Powerful Adsorbents and Fluorescent Probes: Highly Efficient Adsorption and Test Strips-Based Fluorimetric Analysis of Curcumin in Urine and Plant Extracts. *Analyst* **2018**, *143*, 392−395.
(49) Duan, Z. Q.; Zhang, C. X.; Qiao, Y. C.; Liu, F. J.; Wang, D. Y.; Wu, M. F.; Wang, K.; Lv, X. X.; Kong, X. M.; Wang, H. Polyhydric Polymer-Functionalized Fluorescent Probe with Enhanced Aqueous Solubility and Specific Ion Recognition: A Test Strips-Based Fluorimetric Strategy for the Rapid and Visual Detection of Fe^{3+} Ions. *Talanta* **2017**, *170*, 306−313.
(50) Fillebeen, C.; Descamps, L.; Dehouck, M.-P.; Fenart, L.; Benaïssa, M.; Spik, G.; Cecchelli, R.; Pierce, A. Receptor-Mediated Transcytosis of Lactoferrin through the Blood-Brain Barrier. *J. Biol. Chem.* **1999**, *274*, 7011−7017.
(51) Qiao, R.; Jia, Q.; Hüwel, S.; Xia, R.; Liu, T.; Gao, F.; Galla, H.-J.; Gao, M. Receptor-Mediated Delivery of Magnetic Nanoparticles across the Blood-Brain Barrier. *ACS Nano* **2012**, *6*, 3304−3310.
(52) Hanada, S.; Fujioka, K.; Inoue, Y.; Kanaya, F.; Manome, Y.; Yamamoto, K. Cell-Based in Vitro Blood-Brain Barrier Model Can Rapidly Evaluate Nanoparticles' Brain Permeability in Association with Particle Size and Surface Modification. *Int. J. Mol. Sci.* **2014**, *15*, 1812−1825.
(53) Ji, B.; Maeda, J.; Higuchi, M.; Inoue, K.; Akita, H.; Harashima, H.; Suhara, T. Pharmacokinetics and Brain Uptake of Lactoferrin in Rats. *Life Sci.* **2006**, *78*, 851−855.
(54) Betzer, O.; Shilo, M.; Opochinsky, R.; Barnoy, E.; Motiei, M.; Okun, E.; Yadid, G.; Popovtzer, R. The Effect of Nanoparticle Size on the Ability to Cross the Blood-Brain Barrier: An in vivo Study. *Nanomedicine (London, U. K.)* **2017**, *12*, 1533−1546.
(55) Liu, D.; Lin, B.; Shao, W.; Zhu, Z.; Ji, T.; Yang, C. In Vitro and in Vivo Studies on the Transport of PEGylated Silica Nanoparticles across the Blood-Brain Barrier. *ACS Appl. Mater. Interfaces* **2014**, *6*, 2131−2136.
(56) Saraiva, C.; Praça, C.; Ferreira, R.; Santos, T.; Ferreira, L.; Bernardino, L. Nanoparticle-Mediated Brain Drug Delivery: Overcoming Blood-Brain Barrier to Treat Neurodegenerative Diseases. *J. Controlled Release* **2016**, *235*, 34−47.
(57) Cai, X. L.; Luo, Y. N.; Zhang, W. Y.; Du, D.; Lin, Y. H. pH-Sensitive ZnO Quantum Dots-Doxorubicin Nanoparticles for Lung Cancer Targeted Drug Delivery. *ACS Appl. Mater. Interfaces* **2016**, *8*, 22442−22450.
(58) Cai, X. L.; Luo, Y. N.; Yan, H. Y.; Du, D.; Lin, Y. H. pH-Responsive ZnO Nanocluster for Lung Cancer Chemotherapy. *ACS Appl. Mater. Interfaces* **2017**, *9*, 5739−5747.
(59) Farrall, A. J.; Wardlaw, J. M. Blood−Brain Barrier: Ageing and Microvascular Fisease-Systematic Review and Meta-Analysis. *Neurobiol. Aging* **2009**, *30*, 337−352.
(60) Wong, A.; Ye, M.; Levy, A.; Rothstein, J.; Bergles, D.; Searson, P. The Blood-Brain Barrier: An Engineering Perspective. *Front. Neuroeng.* **2013**, *6*, 1−22.

DOI: 10.1021/acsabm.8b00502
ACS Appl. Bio Mater. 2018, 1, 1687−1694